THE JOURNAL OF BIOLOGICAL CHEMISTRY Vol. 277, No. ??, Issue of ???? ??, pp. 1–xxx, 2002
 Printed in U.S.A.

Fibroblast Growth Factor-10 Is a Mitogen for Urothelial Cells*

Received for publication, February 19, 2002
Published, JBC Papers in Press, March 28, 2002, DOI 10.1074/jbc.M201658200

Shelly Bagai‡, Eric Rubio‡, Jang-Fang Cheng§, Robert Sweet‡, Regi Thomas‡¶, Elaine Fuchs‖, Richard Grady‡, Michael Mitchell‡**, and James A. Bassuk‡**‡‡**

*From the §Department of Genome Sciences, Ernst Orlando Lawrence Berkeley National Laboratory, Berkeley, California 94720, the ‖Department of Molecular Genetics and Cell Biology, Howard Hughes Medical Institute, University of Chicago, Chicago, Illinois 60637-4800, the **Division of Pediatric Urology, Children's Hospital and Regional Medical Center, Seattle, Washington 98105, and the ‡Department of Urology, University of Washington School of Medicine, Seattle, Washington 98195*

Fibroblast growth factor (FGF)-10 plays an important role in regulating growth, differentiation, and repair of the urothelium. This process occurs through a paracrine cascade originating in the mesenchyme (lamina propria) and targeting the epithelium (urothelium). *In situ* hybridization analysis demonstrated that (i) fibroblasts of the human lamina propria were the cell type that synthesized FGF-10 RNA and (ii) the *FGF-10* gene is located at the 5p12-p13 locus of chromosome 5. Recombinant (r) preparations of human FGF-10 were found to induce proliferation of human urothelial cells *in vitro* and of transitional epithelium of wild-type and FGF7-null mice *in vivo*. Mechanistic studies with human cells indicated two modes of FGF-10 action: (i) translocation of rFGF-10 into urothelial cell nuclei and (ii) a signaling cascade that begins with the heparin-dependent phosphorylation of tyrosine residues of surface transmembrane receptors. The normal urothelial phenotype, that of quiescence, is proposed to be typified by negligible levels of FGF-10. During proliferative phases, levels of FGF-10 rise at the urothelial cell surface and/or within urothelial cell nuclei. An understanding of how FGF-10 works in conjunction with these other processes will lead to better management of many diseases of the bladder and urinary tract.

AQ: A

The uroepithelial lining of the urinary bladder is a dynamic structure that maintains a barrier to prevent egress of urine and pathogens from the lumen of the bladder. This multilayered urothelia exhibits two hallmark characteristics: an ability to change shape during distension and contraction and a remarkable regenerative capability. Under normal conditions, the urothelium exhibits the slowest turnover of mammalian epithelia (1). During the initial response to injury, the bladder up-regulates the expression of mitogenic growth factors, a process that initiates several rounds of urothelial basal cell proliferation (2, 3). Unlocking the mechanisms responsible for urothelial growth and differentiation is critical to understanding both normal and abnormal bladder pathology. The subsequent modulation of these processes may allow us to improve management of urinary tract abnormalities and inflammatory processes in children and neoplasms and injury in adults. An understanding of these processes may lead to points of potential pharmacological interaction in many disease processes in the bladder.

Heparin-binding growth factors define a group of polypeptides that function as mitogenic signals to urothelial cells. For this group, *in vitro* studies have shown that incorporation of [^{3}H]thymidine into the cellular DNA of human urothelial cells can be stimulated by an epidermal growth factor-like polypeptide (4, 5) or fibroblast growth factor (FGF)[1]-1 (6). Although paracrine pathways for mesenchymally derived FGF-7 have been proposed to initiate mitogenic signaling from the FGF-signal transduction complex at the basolateral face of transitional epithelium (3, 7), the precise mechanisms that describe this process have yet to be elucidated. Systemic administration of FGF-7, also known as keratinocyte growth factor (8), into humans (9) and animals (10, 11), results in proliferation of epithelial lining of the oral cavity (9) and bladder urothelium (7, 10, 11).

Fn1

The importance of mesenchyme to bladder development has been demonstrated in elegant studies where embryonic bladder is placed in direct contact with urogenital sinus mesenchyme, the bladder epithelium differentiates into glandular epithelium that resembles prostatic epithelium (12–14). Insights into the role of FGF-7 in mesenchymal-epithelial cross-talk comes from studies with FGF7-null mice. These mice exhibit the following phenotypes: (i) a matted fur appearance due to a defect in cells giving rise to the hair shaft (15) and (ii) reduction of the intermediate cell layers of bladder urothelium (16). Another abnormal feature noted in FGF-7 null mice is reduced kidney size in proportion to body weight. It has been demonstrated that FGF-7 regulates nephron number and ureteric bud growth (17), thus potentially involving it in the development of congenital anomalies of the urethra and disorganization of the trigone (18).

Interestingly, despite defects in hair follicle, bladder wall, and ureteric bud differentiation, FGF7-null mice appear developmentally normal and fertile (15). One potential source of a

* The costs of publication of this article were defrayed in part by the payment of page charges. This article must therefore be hereby marked "*advertisement*" in accordance with 18 U.S.C. Section 1734 solely to indicate this fact.

The nucleotide sequence(s) reported in this paper has been submitted to the GenBank™/EBI Data Bank with accession number(s) ■■■■.

¶ Current address: Discovery Biology, Bracco Research USA, 305 College Rd. East, Princeton, NJ 08540.

‡‡ To whom correspondence should be addressed: University of Washington, Dept. of Urology, Box 356510 Seattle, WA 98195. Tel.: 425-776-2915; Fax: 425-744-1218; E-mail: bassuk@u.washington.edu.

[1] The abbreviations used are: FGF, fibroblast growth factor; rFGF10-His, recombinant fibroblast growth factor-10 that contains a C-terminal hexamer of histidine residues; FGFR2IIIb, the IIIb splice variant of the *fibroblast growth factor receptor 2* gene; FGFRTK, fibroblast growth factor receptor tyrosine kinase; kbp, kilobase pair(s); STAT, signal transducers and activators of transcription; MOPS, 4-morpholinepropanesulfonic acid; BAC, bacterial artificial chromosome; PBS, phosphate-buffered saline; RT, reverse transcriptase; Ni-NTA, nickel-nitriloacetic acid; FGFR, fibroblast growth factor receptor; JAK, Janus kinase.

AQ: S

compensatory pathway is the polypeptide product of the *FGF-10* gene that is 51% identical to FGF-7 at the amino acid level. During embryonic development, FGF-10 is expressed preferentially in the lungs and prospective limb mesenchyme. It appears to be a key factor in the initial limb budding and continuous limb bud outgrowth of mice. FGF-10 null mice lack limbs and lungs, indicating that FGF-10 is absolutely essential for normal organogenesis and viability during development (19).

In this report, we describe the structure of the human *FGF-10* gene and demonstrate that this gene is transcriptionally active in fibroblasts of the bladder lamina propria. Recombinant preparations of human FGF-10 were active in proliferation assays of human urothelial cells through a pathway that involves a novel form of the FGFR2IIIb receptor. The recombinant protein was mitogenic for bladder urothelium in wild-type and FGF7-null mice and is likely to function through the same receptor as its close relative FGF-7 does.

EXPERIMENTAL PROCEDURES

Materials—Human urinary bladder cDNA was purchased from Invitrogen (Carlsbad, CA). Keystone Laboratories (Foster City, CA) synthesized oligonucleotide primers. Perfectly Blunt Cloning Kit, *Escherichia coli* strains BL21(DE3), BL21*trxB*(DE3), and AD494(DE3) competent cells, plasmid pET21b, and carbenicillin were all obtained from Novagen (Madison, WI). Restriction enzymes, *Xho*I and *Nco*I, T4 DNA ligase, and *Taq* polymerase were all purchased from Roche Molecular Biochemicals (Indianapolis, IN). Ni-NTA metal-chelate affinity resin was purchased from Qiagen Inc. (Chatsworth, CA). HiTrap Heparin-Sepharose affinity columns were acquired from Amersham Biosciences (Piscataway, NJ). Precast SDS-PAGE gels and the Amplified Alkaline Phosphatase ImmunoBlot Assay detection system were purchased from Bio-Rad. Kanamycin and tetracycline were purchased from Calbiochem (La Jolla, CA). AQ: B

Isolation and Dideoxy Sequencing of Bladder FGF-10—Adult human urinary bladder cDNA was used as a template for *Taq* polymerase in a polymerase chain reaction (PCR). One pair of oligonucleotide primers were synthesized: "*Nco*I," 5′-catccggatccatggctcttggtcaggacatg-3′, and "*Xho*I," 5′-actctccggctactcgagtgagtggaccaccat-3′. These oligonucleotide primers were 32 and 33 bases in length, respectively, and were designed to partially anneal to FGF-10 cDNA. The non-complimentary oligonucleotide primer sequence contained sites for the restriction endonucleases *Nco*I or *Xho*I. The following PCR parameters were used: 1 cycle at 95 °C for 12 min; 40 cycles at 95 °C, 50 °C, and 72 °C for 1 min each; 1 cycle at 72 °C for 12 min; and 1 cycle at 4 °C. After the PCR amplification was finished, 10 μl of the 50-μl reaction was fractionated by 1.5% agarose gel electrophoresis in TBE (100 mM Tris, 90 mM boric acid, 1 mM EDTA). The gel was stained with SYBR Green I for 1 h. No DNA bands at the expected size of 525 bp were observed due to low yields. Therefore, 2 μl of the original PCR reaction was used in a reamplification. The conditions for this PCR were as follows: 95 °C for 12 min; 95 and 56 °C for 30 s each for 40 cycles; 72 °C for 10 min and hold at 4 °C. Subsequent agarose gel electrophoresis yielded the expected 525-bp PCR-DNA product. The band at 525 bp was excised from the gel and DNA was extracted and recovered by an ion-exchange spin column (Roche Molecular Biochemicals). The insert cDNA was ligated into a pSTBlue-1 plasmid via blunt ends with T4 ligase. This high copy, recombinant plasmid, was transformed into NovaBlue competent *E. coli* (Novagen). Subsequent growth at 37 °C on agar plates that contained Luria Broth (LB), 50 μg ml^{-1} carbenicillin, and 15 μg ml^{-1} kanamycin yielded recombinant colonies that were analyzed by colony-PCR to determine the presence of the appropriate insert and its orientation. Vector-specific oligonucleotide primers for the T7 and SP6 promoters were annealed to 10 μl of each colony DNA and *Taq* polymerized via the following conditions: 1 cycle at 94 °C for 12 min; 35 cycles at 94 °C (1 min), 55 °C (1 min), 72 °C (2 min); 1 cycle at 72 °C for 5 min; and 1 cycle at 4 °C (hold). The PCR-DNA product was resolved by gel electrophoresis and visualized by fluorescence staining with SYBR Green I. Colonies that yielded PCR-DNA products of 525 bp were grown in LB that contained 50 μg ml^{-1} carbenicillin. Recombinant plasmid DNA was isolated from 3 ml of culture by ion-exchange spin-columns (Qiagen). Glycerol stocks for cultures that displayed the correct insert were prepared and stored at −20 °C and at −80 °C. Both strands of insert cDNAs were characterized by automated, fluorescent dideoxy sequencing with an Applied Biosystem's ABI377XL DNA sequencer. After sequence analysis and comparison to human lung FGF-10 cDNA, this recombinant plasmid was termed pSTBlue-FGF10.

Cloning into Bacterial Expression Vector—Six micrograms of pSTBlue-FGF10 were digested with restriction endonucleases *Nco*I and *Xho*I and resolved by agarose gel electrophoresis. DNA was extracted from the 525-bp band and ligated to the expression plasmid pET-21d, previously prepared by digestion with *Nco*I and *Xho*I and dephosphorylation with shrimp alkaline phosphatase (Roche Molecular Biochemicals). Subsequent ligation into BL21*trxB*(DE3) *E. coli* and propagation yielded the recombinant expression plasmid pET21d-FGF10. The cells were plated and selected via carbenicillin (50 μg/ml) resistance conferred by the recombinant plasmid. The stable cultures were propagated from frozen glycerol stocks.

Growth and Expression of recombinant FGF-10 in E. coli—For 2–10-liter cultures, the following procedure was used. A single recombinant culture was grown in 50 ml if the LB (manufactured from peptone derived from meat to eliminate lactose that would ordinarily be found in peptone derived from milk), 50 μg ml^{-1} carbenicillin, 0.2% (w/v) glucose with an optical density at $A_{600\ nm}$ reached ~0.4–0.6. This culture was stored overnight at 4 °C. The following day, the cells were collected via centrifugation at 5,000 × *g* and resuspended in 4 ml of LB that contained antibiotic and glucose. Each of four flasks that contained 500 ml of medium was inoculated with 1 ml of resuspended culture. rFGF-10 RNA synthesis was induced by addition of isopropyl-1-thio-β-D-galactopyranoside to a final concentration of 1 mM. After 3 h, cells were collected by centrifugation at 5,000 × *g* at 4 °C and frozen at −20 °C. The cells were lysed with lysis buffer (Bug Buster, Novagen) that was supplemented with protease inhibitors (Complete, Roche Molecular Biochemicals). Soluble and insoluble materials were separated by centrifugation at 16,000 × *g* at 4 °C. The soluble extracts were treated according to the method described below. AQ: C

Isolation and Characterization of rFGF10-His—Soluble extracts were dialyzed against Buffer A (0.2 M LiCl, 50 mM Tris-HCl (pH 7.5)) overnight at 4 °C. The soluble extract was centrifuged at 16,000 × *g* at 4 °C to remove insoluble debris. The clarified sample was loaded onto either metal-chelate affinity resins (below) or pre-equilibrated HiTrap-Heparin columns (Amersham Biosciences) and washed until the flow-through displayed a optical density of <0.01 A_{280}. The column was developed with step gradients of 0.5, 1.0, and 1.5 M LiCl. rFGF10-His eluted at a salt concentration of 1.5 M LiCl. AQ: D

Alternatively, rFGF-His was isolated by Ni-NTA metal-chelate affinity chromatography (Qiagen). Soluble extracts were dialyzed against Buffer A (above) that contained 50 mM imidazole for 1 h at 4 °C. The slurry was poured into a chromatography column and allowed to settle at 1 × *g*. The column was developed with buffer B (0.1 M NaH_2PO_4, 0.5 M NaCl, 0.05 M Tris-HCl) at 3 different pH values: 20 column volumes of buffer A at pH 8.0, 20 volumes at pH 6.0, and 10 volumes at pH 5.3. Five-ml fractions were collected. The column eluate was monitored at 280 nm with a Pharmacia Uvicord spectrophotometer connected to analog-to-digital boards of a Pentium-based computer running Rainin Dynamax Chromatography software.

Preparations of rFGF10-His used in tissue culture or animal experiments were evaluated for bacterial endotoxin content by the *Limulus* amebocyte lysate assay (20). Samples and standards were incubated with lysate for 10 min at 37 °C in a microtiter plate and subsequently with Ac-Ile-Glu-Ala-Arg-*p*-nitroaniline for 6 min. The reaction was terminated by the addition of glacial acetic acid to a final concentration of 8.3% (v/v). The release of *p*-nitroaniline was measured photometrically by the absorbance at 405 nm.

Electrophoresis and Immunoblotting—Protein samples were prepared by centrifugal concentration (Microcon-10, Amicon) or by precipitation with trichloroacetic acid (20%). Samples were fractionated by 15% polyacrylamide electrophoretic gels that contained 0.1% SDS, stained with Gel Code Blue (Pierce), and destained with deionized water. Protein samples were fractionated in parallel gels, electrotransferred to nitrocellulose membranes of 0.2-μm porosity, and reacted with goat antibodies specific for human FGF-10 (number AF345, R&D Systems, Minneapolis, MN) or with mouse antibodies specific for C-terminal His_6 (number R930–25, Invitrogen, Carlsbad, CA). Detection of bound antigen-IgG complexes was accomplished with signal amplification systems based on either colorimetric visualization of bands or enhanced chemiluminescence. AQ: E

Amino Acid Sequencing of rFGF10-His—A preparation of rFGF10-His was electrophoresed and transferred to polyvinylidene difluoride membrane in 10 mM MOPS (pH 11.0) that contained 20% (v/v) methanol for 30 min at 300 mA. The transferred protein was visualized by staining with Coomassie Brilliant Blue R-250, excised from the polyvinylidene difluoride membrane, and subjected to Edman degradation.

In Situ Hybridization—Bacterial artificial chromosome (BAC) DNA

was isolated using a alkaline-lysis minipreparation (21). Human metaphase chromosome spreads were generated from peripheral blood lymphocytes according to the protocol previously described (22). To identify additional BACs (CTD-2007E21, CTD-2050F3, CTD-2309D9, and CTD-2313P20), the following FGF10 cDNA oligonucleotide primers were synthesized: FGF10.1.fwd, 5′-CACATTGTGCCTCAGCCTTT-3′ and FGF10.1rev 5′-ACGGGCAGTTCTCCTTCTTG-3′. These primers were used in the following PCR reaction: 94 °C (2 min), 60 °C (30 s), and 72 °C (1 min) for 1 cycle; 94 °C (20 s) and 72 °C (20 s) for 35 cycles. In two-color fluorescent *in situ* hybridization experiments, BAC CTD-2191F10 that is located near the telomere of 5p was used as a control to mark chromosome 5. Sequence of this BAC is available through GenBank™ (number AC022130) and contains the sequence of the marker D5S678 which was mapped previously to 5pter (23). Approximately 15 ng each of the control and the test DNA were labeled: the control with dioxigenin-11-dUTP (Roche Molecular Biochemicals) and the test DNA with biotin-14-dCTP in a random priming reaction using the BioPrime kit (Invitrogen). The labeled BAC DNA was denatured in an 11-μl mixture containing 10 μg of salmon sperm DNA, 1 μg of human Cot-1 DNA, 20% formamide, 6% dextran sulfate, and 0.6 × SSC (20 × SSC is 300 mM NaCl, 30 mM sodium citrate, pH 7.5) at 76 °C for 10 min and then incubated at 37 °C for 1 h before being added to a slide of the metaphase chromosomes. Hybridization was conducted at 37 °C for 24 h. The slides were then washed three times with prewarmed 50% formamide; once with 2 × SSC; once with 0.2 × SSC; and twice with PN buffer (100 mM Na_2HPO_4, 20 mM NaH_2PO_4, and 0.5% IGEPAL CA-630 (Sigma)). Each wash was for 10 min at 42 °C with periodical agitation of slides in Coplin jars. All following steps were conducted at room temperature in the dark. The slides were blocked with PNM buffer (PN buffer that contained 5% w/v nonfat dried milk and 0.02% sodium azide) for 10 min and then treated with 2.5 μg/ml avidin-fluorescein isothiocyanate (Vector Laboratories A-2011) and 2 ng ml^{-1} of anti-digoxigenin rhodamine (Roche Molecular Biochemicals) in PNM buffer for 30 min. The slides were washed twice in PN buffer for 20 min, blocked with PNM buffer for 10 min, and treated with 5 μg ml^{-1} of fluorescein isothiocyanate-conjugated anti-avidin antibody (Vector Laboratories SP-2040) and 7.5 μg ml^{-1} of Texas Red-conjugated anti-sheep IgG antibody (Vector Laboratories TI-6000) in PNM buffer for 30 min. The slides were again washed twice in PN buffer for 20 min. The slides were then dried and stained with DAPI for 10 min before being viewed under a fluorescent microscope. For colorimetric *in situ* hybridization to visualize the cell type that synthesizes FGF-10, a previously published procedure was followed (24).

In Vitro Propagation of Human Urothelial Cells—Four criteria were used to select cultures of normal cells for use in our experiments: 1) initial plating density of 4×10^4 cells cm^{-2} must yield a near-confluent plate in 7–10 days; 2) cobblestone morphology with giant (suprabasal) cells scattered throughout; 3) positive and negative reactivity with anti-cytokeratin and anti-FGF7 IgG, respectively; and 4) >10-fold increase in [^{3}H]thymidine uptake in growth *versus* starved medium conditions (see below). To meet these criteria, we modified a published procedure (25) as follows. Surgical tissue (0.5–4 cm^2) from renal pelvis, ureter, or urinary bladder was incubated 16–24 h in 0.1% EDTA, 1 × Hank's salt solution, 10 mM Hepes (pH 7.8) at 4 °C. After washing, urothelial sheets were teased away from the submucosa with the aid of a dissecting microscope. Urothelium was minced, incubated with type IV collagenase, washed, and grown in serum-free medium in T25-cm^2 Primaria tissue culture flasks. Cultures were passaged when they achieved 70–90% confluent. Cultures were used for experiments between passages 2 and 6. Cultures at passage 3–4 were frozen in liquid nitrogen, and after thawing, cells appeared healthy and grow rapidly.

[^{3}H]Thymidine Incorporation Assays of Urothelial Cell Proliferation—Primary Human ureter epithelial cells were grown and passaged in Keratinocyte Basal Media-2 (Clonetics, Bio-Whittaker). At passage three, the cells were plated at a density of 1.5×10^4 cells per well onto 96-well Primaria tissue culture plates and incubated overnight at 37 °C, 5% CO_2, resulting in 100% confluence the following day. The medium was then changed to Keratinocyte Basal Labeling Media (Clonetics, Bio-Whitakker) without bovine pituitary extract, epidermal growth factor, and thymidine supplements and incubated overnight at 37 °C, 5% CO_2. This was done to render the cells quiescent as verified by comparison of counts/min incorporated by quiescent cells relative to growing cells. Subsequently, the cells were treated with various concentrations of rFGF10-His, in the presence of heparin (5 μg ml^{-1}) and incubated for 20 h at 37 °C, 5% CO_2. The cells were pulsed with 0.5 μCi well^{-1} of [*methyl*-^{3}H]thymidine (925 GBq/mmol, Amersham Biosciences) for 4 h at 37 °C, 5% CO_2. The cells were rinsed twice with phosphate-buffered saline (pH 7.4) and solubilized with 25 μl of 0.1 N NaOH. The cell lysate was transferred to a Whatman GF/C filter paper by a vacuum transfer harvester. The amount of incorporated [^{3}H]thymidine was measured by the Packard TopCount NXT microplate scintillation counter.

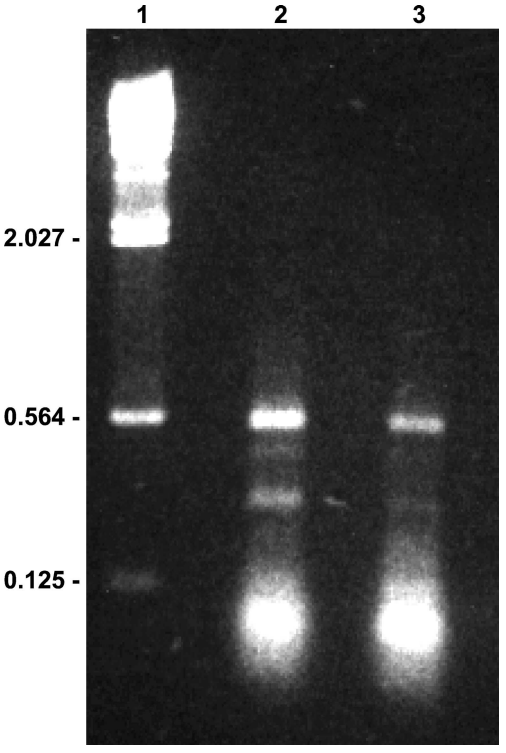

FIG. 1. **Agarose gel electrophoresis of human urinary bladder FGF-10 cDNA.** *Lane 1*, *Hin*dIII markers are indicated to the *left* of the figure in kbp. *Lane 2*, RT-PCR DNA products encoding FGF-10 from oligonucleotide primers designed to generate rFGF10-His. *Lane 3*, RT-PCR DNA products from oligonucleotide primers designed to generate wild-type rFGF-10. Shown is the fluorescent image generated by photography of the gel stained with Sybr Green I. The band at ~545 bp corresponds to FGF-10 cDNA.

In Vivo Administration of rFGF10-His to Mice—A freshly prepared solution of rFGF10-His that contained 5 μg ml^{-1} heparin was dialyzed against phosphate-buffered saline (PBS) (120 mM NaCl, 2.7 mM KCl, 4 mM NaH_2PO_4 (pH 7.4)) for 15 h at 4 °C. The solution was then passed through a 0.2-μm sterile filter into 1-ml aliquots of 270 μg and stored at −20 °C. Gel electrophoresis and Western blot analysis confirmed the presence of isolated rFGF10-His prior to use. One ml that contained 270 μg of rFGF10-His was administered via intraperitoneal injection into 5 wild-type C57BL/6J and 5 FGF7-null/C57BL/6J mice daily for 14 days and compared with 5 wild-type and 5 FGF7-null/C57BL/6J mice who received intraperitoneal injection of 1 ml of PBS. On day 15, the animals were euthanized and their bladders were harvested and secured in anatomical position on a paraffin block. The specimens were placed in Methyl-Carnoy's fixative solution for 24 h and subsequently transferred to PBS. The specimens were embedded in paraffin and 5-μm thick cross-sections of the bladder were generated.

Histological and Immunohistochemical Procedures—Adjacent bladder sections were stained with hematoxylin and eosin, Masson's trichrome solution, or rabbit antibodies specific for the proliferation marker Ki-67. The procedure for Ki-67 immunostaining has been described (26).

RESULTS

Isolation and Sequence Analysis of FGF-10 cDNA from Human Urinary Bladder—A partial cDNA fragment that encoded the mature, secreted form of FGF-10 was isolated from a human urinary bladder cDNA library by reverse transcription (RT) and PCR. Fig. 1 demonstrates that the RT-PCR reaction yielded a 545-bp DNA product in agreement with the size predicted from the mRNA encoding human lung FGF-10 (GenBank™ accession AB002097).

The 545-bp FGF-10 cDNA insert was subcloned into the high

balt3/bc-bc/bc-bc/bc2202/bc8842-02a eichelbt S=7 30/4/02 19:47 **4/Color Figure(s) 2,3,6-8** ARTNO: M201658200

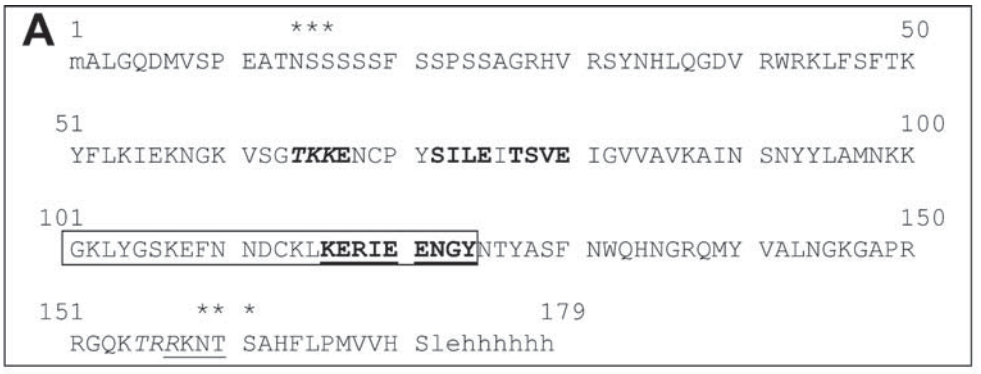

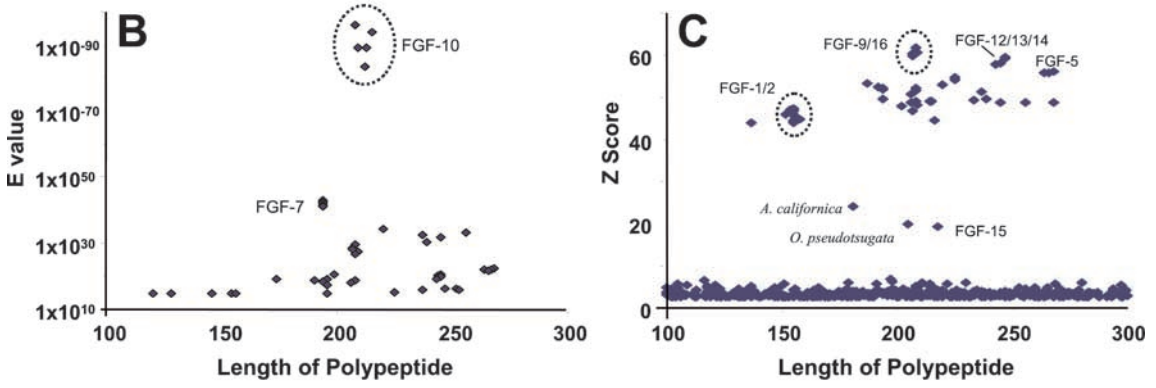

AQ: P

FIG. 2. **Sequence analysis of human FGF-10.** *A,* primary structure of recombinant FGF10-His. The amino acid sequence for rFGF10-His was deduced from data derived from the dideoxy sequencing of the PCR-DNA product shown in Fig. 1, *lane 2*. Not part of the wild-type sequence (*capital letters*) are the formyl-methionine at the N terminus of the sequence, and the Leu, Glu, and six His residues at the C terminus. The His-hexamer at the C terminus was engineered to allow easy differentiation during biological assays, and to allow isolation of the protein using nickel-chelate affinity chromatography. *Asterisks* indicate sites of *N*-linked glycosylation. *Underlined* residues represent cAMP- and cGMP-dependent protein kinase phosphorylation sites. *Bold* residues indicate putative casein kinase II phosphorylation sites. *Italicized* residues indicate protein kinase C phosphorylation sites. *Bold underlined* residues represent the tyrosine kinase phosphorylation site. The *boxed* sequence is the heparin signature. *B,* comparison of bladder FGF-10 sequence to known protein sequences. BLASTP version 2.0 analysis (34) was performed with the 170-amino acid coding region of human urinary bladder FGF-10 as a query (*capital letters* in *panel A*). Sequences to which FGF-10 was compared with included non-redundant entries derived from the GenBank™, EMBL, DDBJ, and PDB databases (www.ncbi.nlm.nih.gov/BLAST). The *ordinate* displays units of Expected (*E*) value, a reference to the statistical significance of the data. *C,* comparison of bladder FGF-10 sequence to known FGF polypeptide growth factor sequences. PROFILE analysis (35) was performed with a profile derived from a multiple sequence alignment of the 20 known members of the human fibroblast growth factor family of protein as a query. Sequences to which the profile was compared with included entries derived from release 38.0 of the Swiss Protein databases through the PROFILESEARCH toolbox of the Wisconsin Package (version 10.0-UNIX) running under release V4.0 878 of the OSF1 operating system. The algorithm calculates the quality score and normalizes the output to polypeptide length (Z score as shown on the ordinate). Z scores >6 are considered statistically significant. *A. californica*, FGF homologue (accession number P41444), *O. pseudotsugata* (accession number O10284). These sequence data are available from GenBank™/EMBL/DDBJ under accession ■■■■.

copy vector pSTBlue1 to form the recombinant plasmid designated pSTBlue1-FGF10. Dideoxy sequencing and sequence analysis of both strands of the insert revealed a 100% match between the two strands. This human urinary bladder cDNA insert exhibited a 99.6% identity match with the coding region for human adult lung FGF-10 mRNA (27). The discrepancy in the cDNA sequence was determined to exist at the wobble position of the codon for Val^{206}. The amino acid Val^{206} is encoded by the bladder codon GTC and by the lung codon GTA. The collective data indicate that the primary structure of the mature, secreted form of human FGF-10 is identical between urinary bladder and lung.

F2

Analysis of Human Urinary Bladder FGF-10 Amino Acid Sequence—Fig. 2*A* displays the deduced amino acid sequence for the recombinant protein. The N terminus was engineered to contain a Met residue to provide a translational initiation codon for *E. coli*. The C terminus was engineered to contain a His-hexamer to provide for purification by nickel-chelate affinity chromatography. The predicted molecular weight and isoelectric point for rFGF10-His is 20,390 and 10.7, respectively.

Fig. 2*A* also displays motifs and sites of post-translational modifications that are predicted to occur in the wild-type FGF-10 sequence. Naturally occurring FGF-10 proteins contain glycosylated residues according to the consensus sequence Asn-Xaa-(Ser/Thr). Residues 14–16 and residues 159–161 are *N*-glycosylation sites on FGF-10 as denoted by *asterisks* in Fig. 2*A*. Amino acids 116–124, underlined, represent cAMP and cGMP-dependent protein kinase phosphorylation sites. Both of these kinases share a preference for phosphorylation of serine or threonine residues found close to at least two N-terminal basic residues. It should be noted that there are many exceptions to this rule. Bold residues 64–67, 72–75, 77–80, and 116–124 indicate putative casein kinase II phosphorylation sites. Casein kinase II is a protein serine/threonine kinase whose activity is independent of cyclic nucleotides and calcium. It prefers serine over threonine, and must have an acidic residue present three residues from the C terminus of the phosphate acceptor site. Italicized residues indicate protein kinase C phosphorylation sites at residues 64–66. Protein kinase exhibits a preference for the phosphorylation of serine or threonine residues found close to the C terminus basic residues. Presence of additional basic residues at the N or C terminus of the target amino acid increases the rate of the phosphorylation reaction. The bold-underlined residues 116–124 indicate the tyrosine kinase phosphorylation site. This phosphorylation site is generally characterized by the presence of a lysine, or an

arginine, seven residues to the N terminus side of the phosphorylation target tyrosine. The boxed residues designate the region of FGF-10 that binds to heparin.

Comparison of Bladder FGF-10 to Known Proteins—We evaluated the relationship between the amino acid sequence of bladder FGF-10 and entries in the sequence databases by two analyses. Fig. 2*B* displays BLASTP analysis that defines the relationship of FGF-10 sequences to all entries in the DNA databases. A group of FGF-7 sequences is most closely related to the FGF-10 query, followed by the remaining members of the FGF family of proteins. A PROFILE analysis of the SwissProt database that was queried with a profile derived from a multiple sequence alignment of the 20 known FGF protein sequences is shown in Fig. 2C. FGF-9 and FGF-16 exhibit the best fit to the input profile, followed by FGF-12/13/14 and FGF-5. Of interest are two sequences from the nucleopolyhedroviruses *Autographa californica* and *Orgyia pseudotsugata* that exhibit Z scores of 24.17 and 19.72, respectively, and a 30 and 26% amino acid sequence identity, respectively, with bladder FGF-10.

Identification and Analysis of the Human FGF-10 Gene—The cDNA coding sequence for human urinary bladder FGF-10 was used to query draft and finished sequences derived from the Human Genome Project. The four matches obtained are summarized in Table I. A 209-bp region of the bladder FGF-10 cDNA was localized to both chromosomes 5 and 6. The match for chromosome 6 is in contrast to a prior report (27) that assigned the gene for *FGF-10* to chromosome 5 based on radioactive hybridization data. To resolve this potential discrepancy between chromosomes 5 and 6, we performed a fluorescent *in situ* hybridization analysis with BAC clones that contained the *FGF-10* gene as a probe. Fig. 3 demonstrates that our probe exhibits a specific hybridization with the 5p12-p13 region (area of blue/green fluorescence) of chromosome 5. Chromosome 5 was identified based on its hybridization to a positive control for the telomere of chromosome 5 that fluoresced bright red. No signal was observed for chromosome 6.

The intron/exon structure of the human *FGF-10* gene was deduced from the 326.749-kbp contig number NT_023098.2 of chromosome 5 (Table II). The gene is at least 52.7 kbp in length. While our current data does not address the precise lengths of the 5′- and 3′-untranscribed regions of the gene, we find that 2 introns divide 3 exons to generate the human FGF-10 mRNA. A 38-residue N-terminal secretory signal sequence (MWKWILTHCASAFPHLPGCCCCCFLLLFLVSSVPVTCQ) resides in exon 1. The AGC codon for Ser (bold, underlined type in Table II) is interrupted by intron 1.

Expression of Recombinant FGF10-His in E. coli—The insert cDNA from pSTBlue1-FGF10 was subsequently ligated into the pET21d expression vector to form the recombinant expression plasmid pET21d-FGF10. The expression of recombinant FGF-10 (rFGF10) protein by transformed *E. coli* was dependent on the addition of 1 mM isopropyl-1-thio-β-D-galactopyranoside, which inactivates the *lac* repressor and allows synthesis of the encoded protein. The expression pattern of rFGF-10 was

TABLE I
Distribution of bladder FGF-10 sequence in the human genome

Chromosome	Match contig segment (kbp)	% Identity (bp/bp)
6	NT_023436.3 (189.354)	100% (209/209)
5	NT_023098.2 (326.749)	100% (209/209)
5	NT_023098.2 (326.749)	100% (188/188)
5	NT_023098.2 (326.749)	100% (104/104)

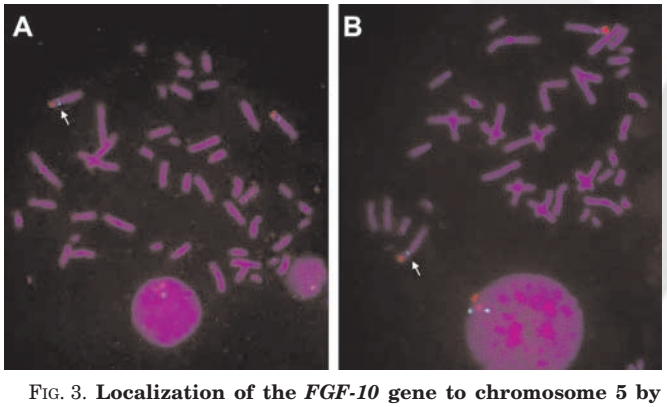

FIG. 3. **Localization of the *FGF-10* gene to chromosome 5 by fluorescence *in situ* hybridization.** BAC clones that contained the *FGF-10* gene were hybridized to two different human chromosome spreads (*A* and *B*)**.** Clones CTD-2313P20 and RP11-703E1 were used as the probe in *panels A* and *B*, respectively. *White arrow* designates positive FGF-10 signal (*blue-green band*). Positive control specific for the 5q telomere of chromosome 5 is the *red band*. *Large circles* are hybridization filter papers that contain cells with interphase DNA.

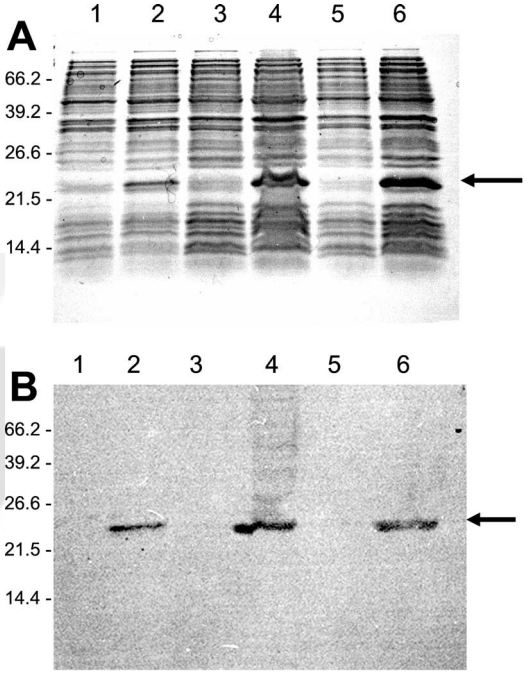

FIG. 4. **Expression of rFGF10-His in *E. coli*.** Aliquots were removed from culture at the indicated times and fractionated by two identical 15% polyacrylamide electrophoretic gels. *A,* GelCode Blue-stained gel. *B*, Western immunoblot. Lanes correspond to both gel and immunoblots. *Lanes 1*, *3*, and *5* are uninduced (0 h) aliquots. *Lanes 2*, *4*, and *6* are isopropyl-1-thio-β-D-galactopyranoside-induced (2 h) samples of the same culture. *Lanes 1* and *2* are *E. coli* strain AD494(DE3); *lanes 3* and *4* are *E. coli* strains BL21(DE3); and *lanes 5* and *6* are *E. coli* strain BL21(DE3)*trxB*. Proteins were transferred to nitrocellulose and detected with a monoclonal antibody specific for C-terminal His-hexamers. *Arrow* denotes the ~24-kDa rFGF10-His.

TABLE II
Intron/exon structure of human FGF-10 gene on chromosome 5

	5′ Region	Exon 1	Intron 1	Exon 2	Intron 2	Exon 3	3′ Region
Size (kbp)	6.062	0.325	36.663	0.104	5.234	0.198	4.107
Sequence of Border	tacaATGTGA	TACAGtaag	TaggCATCCTG	GGCTCAgtaa	gcagAAAGAA	TCATAGagga	
	MetTrp	Tyr*Se*	*r*IleGlu	GlySer	LysGlu	Ser***	

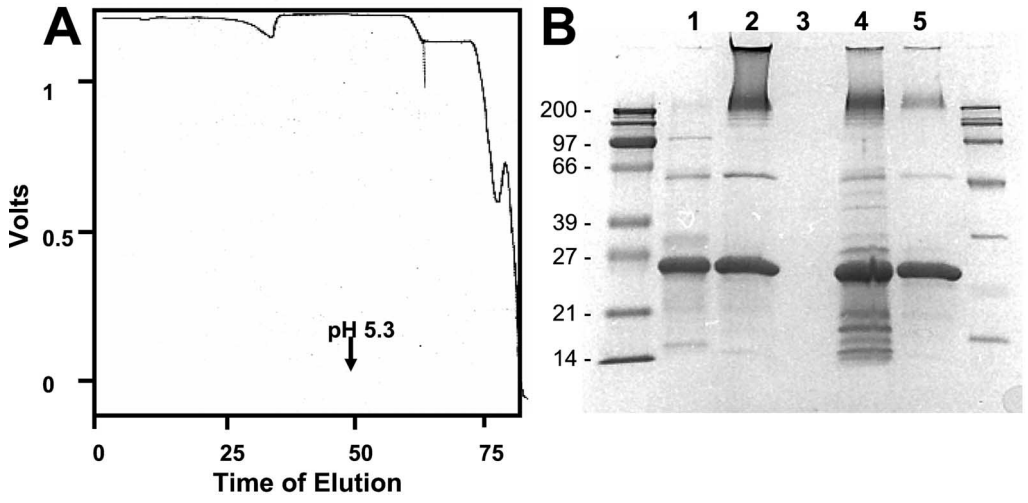

FIG. 5. **The C-terminal His tag of rFGF10-His does not interfere with heparin binding.** *A,* elution from Ni-NTA resin. Soluble bacterial lysates were applied to a Ni-NTA column at pH 8.0 in 0.1 M NaH_2PO_4, 0.5 M NaCl, 0.05 M Tris-HCl. Contaminating proteins were removed with a pH 6.0 wash in the same buffer. Specific elution of soluble, monomeric rFGF10-His was accomplished with pH 5.3. Time of elution is in minutes. *B,* sequential chromatography of rFGF10-His on Ni-NTA and heparin affinity resins. A two-liter culture of *E. coli* containing the recombinant plasmid was grown in culture. The soluble extract was divided into equivalent fractions and subjected to sequential chromatography. *Lane 1*, rFGF10-His isolated from a Ni-NTA affinity chromatography column. *Lane 2*, sample from *lane 1* was applied to a HiTrap-heparin column at 0.2 M LiCl, washed with 0.5 and 1.0 M LiCl, and eluted with 1.5 M LiCl. *Lane 4*, rFGF10-His was isolated first from the soluble extract using a heparin column. *Lane 5*, sample from *lane 4* was sequentially applied to a Ni-NTA chromatography column. The 15% polyacrylamide gel was stained with GelCode Blue. Molecular markers on the *left* are in kDa.

AQ: R

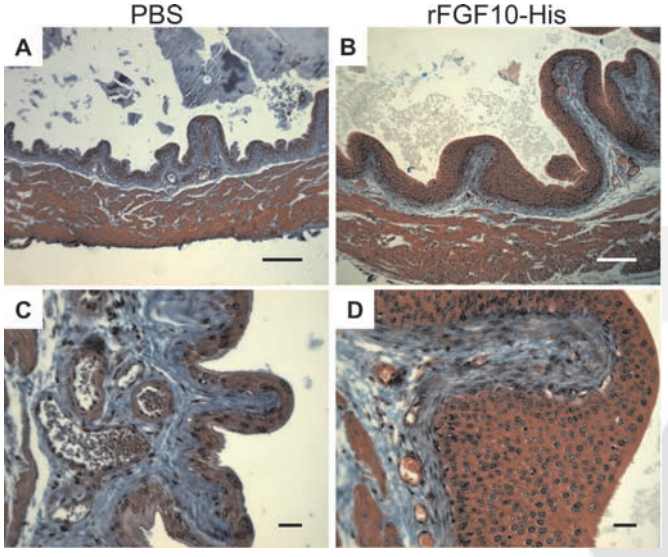

FIG. 6. **Induction of expansion and proliferation of transitional epithelia in bladders of wild-type mice by rFGF10-His.** Vehicle (*A* and *C*) or rFGF10-His (*B* and *F*) was administered via intraperitoneal injection into wild-type mice for 14 days. Shown are fixed sections stained with Mason's Trichrome reagent (*A-D*). Magnifications: ×100, *bar* = 100 μm (*A* and *B*); ×400, *bar* = 20 μm (*C* and *D*).

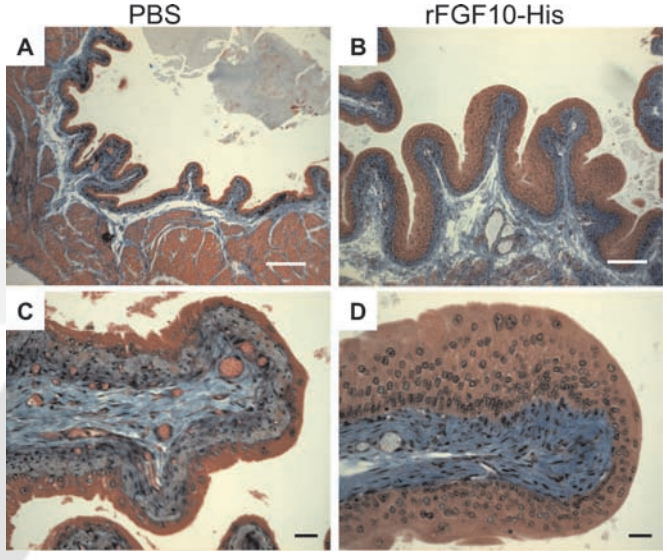

FIG. 7. **Induction of expansion and proliferation of transitional epithelia in bladders of FGF7-null mice by rFGF10-His.** Vehicle (*A* and *B*) or rFGF10-His (*B* and *D*) was administered via intraperitoneal injection into FGF7-null mice for 14 days. Shown are fixed sections stained with Mason's Trichrome reagent (*A-D*). Magnifications: ×100, *bar* = 100 μm (*A* and *B*); ×400, bar = 20 μm (*C* and *D*).

analyzed by polyacrylamide electrophoretic gels that contained sodium dodecyl sulfate, and by Western immunoblotting. Fig. 4*A* displays an electrophoretogram with samples collected from three different strains of *E. coli* prior to and after a 2-h induction with isopropyl-1-thio-β-D-galactopyranoside. The stained protein bands at 24 kDa was notably larger in amount in the 2-h induced sample (*lanes 2*, *4*, and *6*) than in the 0-h uninduced sample (*lanes 1*, *3*, and *5*). This level of induction was consistently observed both in the 25-ml pilot cultures and 2-liter cultures. Levels of expressed rFGF-10 reached a maximum by 3.5 h.[2] An identical electrophoretic gel was transferred to nitrocellulose and probed with a monoclonal antibody specific for the C-terminal His-hexamers. Fig. 4*B* demonstrates that the rFGF-10 protein present at 24 kDa was immunoreactive with an antibody specific for C-terminal His-hexamers. We have designated this protein as rFGF10-His. Comparable results were obtained with polyclonal antibodies raised against FGF-10.[2] The collective results prove that rFGF10-His was expressed by BL21(DE3) *E. coli.*

F4

Fn2

AQ: L

Isolation and Characterization of rFGF10-His—The recombinant protein was found to be expressed in both a soluble and insoluble form by *E. coli.* The soluble form of rFGF10-His was readily recovered from culture lysates by affinity chromatography over heparin- or nickel- containing resins. Fig. 5*A* displays the elution profile of rFGF10-His from nickel-nitriloacetic acid

F5

AQ: T

[2] S. Bagai, E. Rubio, J-F. Cheng, R. Sweet, R. Thomas, E. Fuchs, R. Grady, M. Mitchell, and J. A. Bassuk, unpublished data.

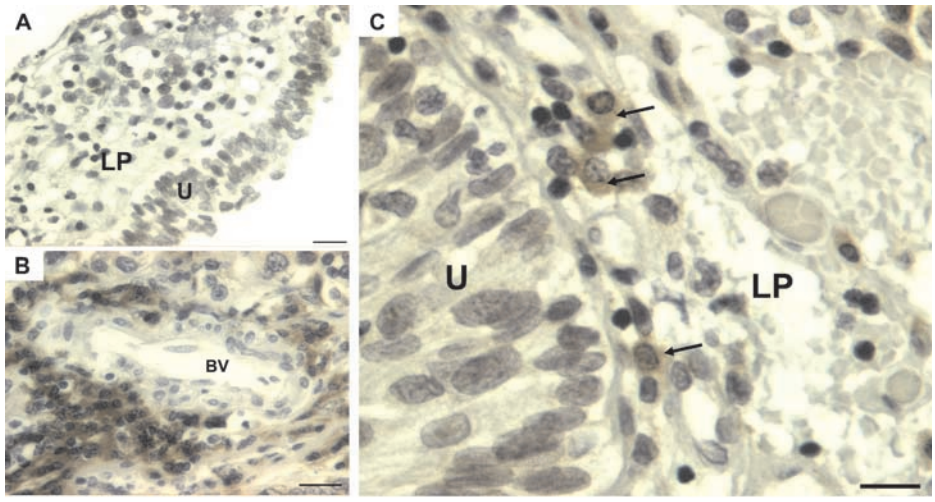

FIG. 8. **Synthesis of FGF-10 mRNA by fibroblasts of the lamina propria.** Sections of human urinary bladder were hybridized to the sense (*panel A*) or antisense (*panels B* and *C*) strands of human urinary bladder FGF-10 cDNA. *Arrows* indicate fibroblasts that stained positive for FGF-10 mRNA. Magnification was ×400. The *bar* is 0.02 mm in length. *U*, urothelium; *LP*, lamina propria; *BV*, blood vessel.

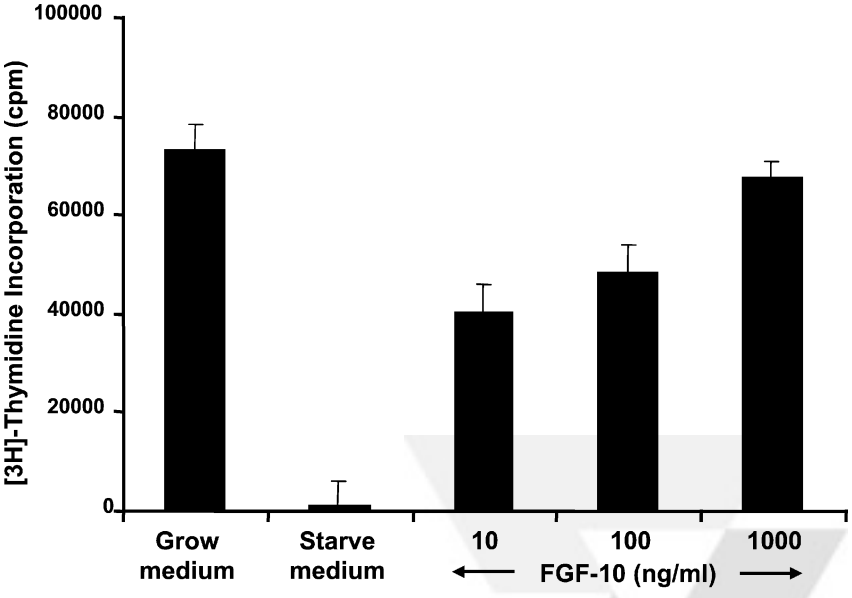

FIG. 9. **Inhibition of human urothelial DNA synthesis by rFGF10-His *in vitro*.** Ureteric urothelial cells were treated with various concentrations of rFGF10-His in the presence of heparin (5 μg ml^{-1}). DNA synthesis was assayed by [^{3}H]thymidine incorporation. Shown is the mean ± S.E.

(Ni-NTA) affinity resins. Protonation of His residues was accomplished by the reduction of column buffer pH to 5.3, a condition that disrupted the interaction of rFGF10-His with the Ni-NTA resin. Electrophoretic analysis of the reduced pH 5.3 fraction is shown in *lane 1* of Fig. 5*B*. The electrophoretic mobility of unreduced rFGF10-His was found to be slightly greater than the mobility of reduced rFGF10-His.[2] This phenomenon is consistent with the soluble form existing in a correctly folded state.

To further address the functionality of the folding of our isolations of rFGF10-His, sequential chromatography on Ni-NTA and heparin resins was performed. The soluble extract from a 2-liter recombinant culture was divided into two portions: one portion was subjected to heparin affinity chromatography and the other portion was fractionated by nickel-chelate affinity chromatography. Fig. 5*B*, *lane 1,* shows the isolated rFGF10-His fraction after one pass of the soluble extract over the Ni-NTA affinity resin. This fraction was dialyzed and applied to a heparin affinity column equilibrated at 0.2 M LiCl. rFGF10-His was eluted with 1.5 M LiCl (Fig. 5*B*, *lane 2*). The reciprocal experiment involved chromatography of the bacterial lysate over heparin affinity resins (Fig. 5*B*, *lane 4*) and sequential chromatography over Ni-NTA resins (Fig. 5*B*, *lane 5*).

Our preparations of rFGF10-His were judged to be intact according to two criteria. 1) The N terminus of rFGF10-His was subjected to amino acid sequencing by Edman degradation. The following sequence was procured: ALGQ(S)MVSPEATN. This sequence is in agreement with the amino acid sequence deduced from dideoxy sequencing of the pSTBlue1 clone that contained the human bladder FGF10-insert (above) and from the deduced amino acid sequence of human lung FGF-10 (GenBank™ accession number AB002097). 2) The presence of the C-terminal His-hexamer was confirmed by binding of rFGF10-His metal-chelate resins (Fig. 5*B*, *lanes 2* and *4*) and immunoreactivity with antibodies specific for C-terminal His-hexamer motifs (Fig. 4*B*).

Mitogenic Activity of rFGF10-His on Urothelial Cells in Vivo—Intraperitoneal injection of rFGF10-His into C57BL/6 wild-type mice for 14 days resulted in marked expansion of urinary bladder transitional epithelium (Fig. 6). While wild-type mice injected with vehicle (PBS) exhibited a normal transitional epithelium comprised of 2–5 layers of urothelial cells (Fig. 6, *A* and *C*), wild-type mice injected with rFGF10-His exhibited up to 20 layers of urothelial cells (Fig. 6, *B* and *D*). This observed uroepithelial expansion was a consequence of proliferation as determined by immunoreactivity of anti-Ki67 immunoglobulins with urothelial cell nuclei.[2] F6

An equally striking, if not greater, expansion was noted in FGF7-null mice injected with rFGF10-His (Fig. 7). Urothelial cells expansion was observed when transgenic mice of the same F7

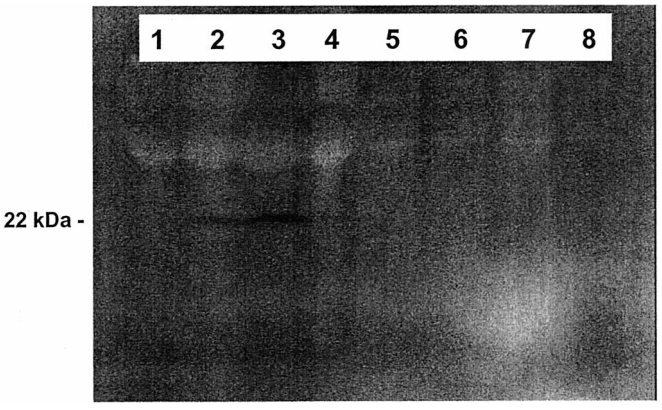

FIG. 10. **Translocation of rFGF10-His to nuclei of human urothelial cells *in vitro*.** rFGF10-His was fed to cells overnight prior to harvesting of nuclei in the presence of protease inhibitors. *Lanes 1*, nuclear fraction from control cells; *2* and *3*, nuclear factor from rFGF10-His-treated cells; *4*, nuclear fraction from rFGF-7-treated cells; *5*, cytoplasmic fraction from control cells; *6* and *7*, cytoplasmic fraction from rFGF10-His cells; *8*, cytoplasmic fraction from rFGF-7-treated cells. Shown is a Western immunoblot that used immunoglobulins specific for human FGF-10. The experiment was visualized with enhanced chemiluminescence or colorimetric development.

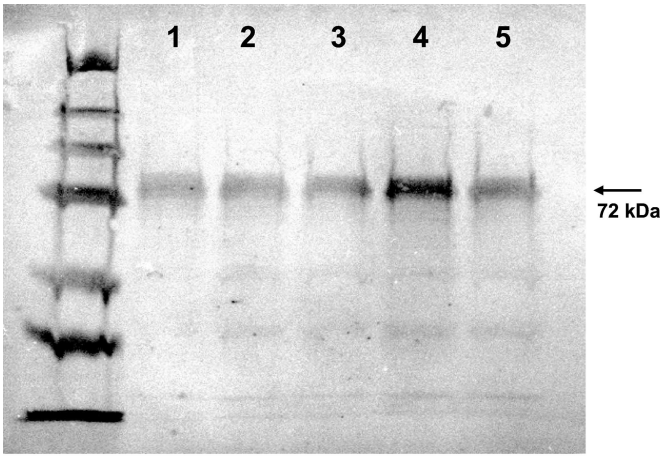

FIG. 11. **Immunoprecipitation of a novel 72-kDa form with an antibody specific for the FGFR2IIIb receptor splice variant.** Human urothelial cells were rendered quiescent for 24 h and then incubated for 15 min with rFGF10-His. Soluble proteins from cytoplasmic extracts were prepared and incubated with anti-FGFR2IIIb antibodies. After recovery with Protein A beads, FGFR2IIIb:IgG complexes were resolved by electrophoresis, transferred to nitrocellulose, and probed with anti-phosphotyrosine antibodies. *Lanes 1* and *2,* cells not fed rFGF10-His. *Lane 3,* cells fed 0.1 μg ml^{-1} rFGF10-His. *Lane 4,* cells fed 0.1 μg ml^{-1} rFGF10-His plus 5 μg ml^{-1} heparin. *Lane 5,* cells fed 0.1 μg ml^{-1} rFGF10-His plus 0.5 μg ml^{-1} heparin. The experiment was visualized with enhanced chemiluminescence.

C57BL/6 background were injected for 14 days with rFGF10-His (Fig. 7, *B* and *D*). In contrast, transgenic mice injected with PBS vehicle exhibited the normal 2–5 layers of cells that is typified by the wild-type animal (Fig. 7, *A* and *C*).

Synthesis of FGF-10 mRNA by Fibroblasts of the Lamina Propria—Bladder FGF-10 cDNA was used to probe the site of synthesis in the bladder. Fig. 8 exhibits the *in situ* hybridization pattern in a biopsy specimen from human bladder. FGF-10 RNA signals were only observed in the lamina propria, there were no signals in the urothelium. Strong signals of FGF-10 RNA synthesis were observed in fibroblasts proximal to blood vessels (Fig. 8*B*) and in fibroblasts just below the urothelial basement membrane (Fig. 8*C*).

Mitogenic Activity of rFGF10-His on Urothelial Cells in Vitro—rFGF10-His stimulated the synthesis of urothelial cell DNA in a concentration-dependent manner (Fig. 9). DNA synthesis was measured by monitoring the incorporation of [^{3}H]thymidine into the DNA of human urothelial cells *in vitro*. Actively dividing cultures (Fig. 9, *growth medium*, 73,000 cpm) were first rendered quiescent by incubation in medium that lacked growth-promoting factors (Fig. 9, *starve medium,* 1,100 cpm). Addition of rFGF10-His to starved cultures induced a rapid and marked increase in uptake of [^{3}H]thymidine. Stimulation of [^{3}H]thymidine uptake was also found to require heparin, omission of this mucopolysaccharide sulfuric acid ester resulted in poor uptake.[2]

Two Mechanisms to Explain the Mitogenic Activity of rFGF10-His—Two pathways were considered to establish how the rFGF10-His signal is transduced from the urothelial cell surface to the urothelial cell nucleus. Fig. 10 (*lanes 2–3*) demonstrates that the growth factor is detected by anti-FGF10 antibodies in nuclear fractions after a 16-h incubation with actively growing cells. Similar results were obtained with anti-His_6 monoclonal antibodies.[2]

rFGF10-His also induced the phosphorylation of tyrosine residues of the bladder isoform of the FGFR2III receptor (Fig. 11). Growth-arrested cultures of human urothelial cells were stimulated with 0.1 μg ml^{-1} rFGF10-His for 15 min. Following detergent-induced cellular lysis, anti-FGFR2IIIb immunoprecipitates were assayed for phosphotyrosine by Western immunoblotting. A significant increase in the tyrosine phosphorylation signal was observed in cells fed rFGF10-His (*lane 4*) over control cells (*lanes 1* and *2*). Increased phosphorylation was dependent on the presence of heparin (*lane 4*, 5.0 μg ml^{-1}). Cells treated with rFGF10-His in the absence of heparin (*lane 3*) or with low levels of heparin (*lane 5*) did not exhibit any increase of phosphorylation over background.

DISCUSSION

Our results provide the first evidence that FGF-10 plays an important role in regulating DNA synthesis of urothelial cells, a crucial process involved in control of growth, differentiation, and repair of the urothelium. This process is described by a complex network of paracrine action that originates in the fibroblasts of the mesenchyme but acts on urothelial cells of the transitional epithelium. Once FGF-10 is synthesized and secreted by these fibroblasts, the growth factor must then traverse the collagenous network of the lamina propria, cross the urothelial cell membrane, interact with the urothelial cell surface, and ultimately trigger a mitogenic event. The mechanisms by which FGF-10 arrives at the cell surface and how its signal is transduced to stimulate progression through the urothelial cell cycle are currently unknown.

The FGF receptor (FGFR) signal transduction complex is comprised by three components: (i) the regulatory polypeptide FGF, (ii) transmembrane tyrosine kinases (FGFRTK), and (iii) heparan sulfate proteoglycans (28). In our *in vitro* model of primary cultures of human urinary bladder urothelial cells, we found that our preparations of recombinant FGF-10 required heparin for activity in assays of FGFRTK activation (*i.e.* phosphorylation of tyrosine residues of bladder FGFRTK) and in assays of [^{3}H]thymidine incorporation. The observed dependence on heparin for FGF-10 activity in assays of DNA synthesis is in agreement with studies with Balb/MK mouse epidermal keratinocytes (29) and human prostate epithelial cells (30). The addition of a C-terminal His hexamer to rFGF10-His did not influence binding of rFGF10-His to heparin affinity resins. This result is significant because the C-terminal region of fibroblast growth factors is crucial for its biological activity and high level protein expression in mammalian cells (31). The identity of the *in vivo* heparan sulfate proteoglycan involved in the FGFR signal transduction complex is not known.

Our results suggest that FGFRTK activation is linked to urothelial cell mitogenesis. We have characterized the urothelial cell FGFRTK activated by incubation with rFGF10-His and have discovered that the 72-kDa bladder FGFR2IIIb isoform is 20 kDa smaller than the canonical FGFR2III polypeptide (KGFR, accession number A45081). While we cannot rule out the possibility of proteolysis during our immunoprecipitation steps, we feel that such degradation is unlikely because of the wide variety of protease inhibitors and cold temperatures we employed during these steps. We favor a variant form that probably arises from alternative splicing, a well recognized phenomenon that generates a complex array of FGFRTK from only 4 *FGFR* genes. The anti-FGFR2IIIb antibody used to immunodetect the 72-kDa bladder isoform is specific for the intracellular/tyrosine kinase domain, thus raising the possibility that one or more of the 3 internal, immunoglobulin-like domains have been deleted. Downstream signaling events have yet to be described, but we believe that extracellular FGF-10 would stimulate receptor-mediated endocytosis and subsequent degradation or recycling. It is plausible that FGF-10 can escape endosomes or lysosomes and reach the nucleus. Indeed, our data support the translocation of rFGF10-His into urothelial cell nuclei. We consider 4 possibilities to explain this translocation phenomenon: 1) a true nuclear localization signal exists, 2) simple diffusion, 3) co-translocation with the receptor for rFGF10-His, or 4) assistance from a carrier protein. Whether nuclear transport is linked to mitogenesis or whether a rFGF10-His::FGFR2IIIb complex comigrates into nuclei is not known. Nuclear localization signals demonstrated for FGF-1 have been identified by us for FGF-10. We are actively working to construct and test such recombinant mutations of rFGF10-His in our system.

Administration of rFGF10-His to mice by intraperitoneal injection was well tolerated, did not lead to complications, and resulted in marked expansion of urothelium. The interaction with the FGFR2IIIb receptor is supported by a high level of mitogenic activity of rFGF10-His in FGF7-null mice. Since both FGF-10 and FGF-7 are known to bind to, activate, and trigger a mitogenic signaling pathway via FGFR2IIIb in prostate epithelium (30), it is reasonable to suppose that the two growth factors compete for the same receptor in uroepithelium. The continued responsiveness of FGF7-null uroepithelium to rFGF10-His suggests that FGFR2IIIb levels are significant and amenable to activation. In the absence of FGF-7, the number of FGF-7 receptors might be increased. Indeed, FGF-10 acts as a major ligand for FGFR2IIIb in mouse multiorgan development because the phenotypes of FGF10-null mice closely mirror the phenotypes of FGFR2IIIb-null mice (32). Signaling would then proceed via the mitogen-activated protein kinase and JAK-STAT pathways (33).

Growth factors such as FGF-10 likely play a critical role in the urothelial response to injury that is secondary to infection, trauma, urinary tract obstruction, and ischemia. They may also be involved in carcinogenesis. Manipulation of the urothelial response via these growth factors may reduce scar formation or accelerate the eradication of infection. The utility of rFGF10-His as a therapeutic agent is therefore promising.

Acknowledgments—We thank Dr. Waldo Fang for a critical reading of the manuscript, Brian Umrysh for invaluable assistance with our mouse colony, and Kimber Cochrane for technical assistance.

REFERENCES

1. Hainau, B., and Dombernowsky, P. (1974) *Cancer* **33,** 115–126
2. Levin, R. M., Wein, A. J., Buttyan, R., Monson, F. C., and Longhurst, P. A. (1994) *World J. Urol.* **12,** 226–232
3. Baskin, L. S., Sutherland, R. S., Thomson, A. A., Hayward, S. W., and Cunha, G. R. (1996) *Lab. Invest.* **75,** 157–166
4. Freeman, M. R., Yoo, J. J., Raab, G., Soker, S., Adam, R. M., Schneck, F. X., Renshaw, A. A., Klagsbrun, M., and Atala, A. (1997) *J. Clin. Invest.* **99,** 1028–1036
5. Chai, T. C., Zhang, C. O., Shoenfelt, J. L., Johnson, H. W. J., Warren, J. W., and Keay, S. (2001) *J. Urol.* **163,** 1440–1444
6. Rebel, J. M., De Boer, W. I., Thijssen, C. D., Vermey, M., Zwarthoff, E. C., and Van der Kwast, T. H. (1994) *J. Pathol.* **173,** 283–291 **AQ: N**
7. Bassuk, J. A., Grady, R., and Mitchell, M. E. (2000) *J. Urol.,* in press
8. Rubin, J. S., Bottaro, D. P., Chedid, M., Miki, T., Ron, D., Cheon, G., Taylor, W. G., Fortney, E., Sakata, H., and Finch, P. W. (1995) *Cell Biol. Int.* **19,** 399–411
9. Danilenko, D. M. (1999) *Toxicol. Pathol.* **27,** 64–71
10. Yi, E. S., Shabaik, A. S., Lacey, D. L., Bedoya, A. A., Yin, S., Housley, R. M., Danilenko, D. M., Benson, W., Cohen, A. M., and Pierce, G. F. (1995) *J. Urol.* **154,** 1566–1570
11. Ulich, T. R., Whitcomb, L., Tang, W., O'Conner, T. P., Tarpley, J., Yi, E. S., and Lacey, D. (1997) *Cancer Res.* **57,** 472–475
12. Donjacour, A. A., and Cunha, G. R. (1988) *Dev. Biol.* **128,** 1–14
13. Neubauer, B. L., Chung, L. W., McCormick, K. A., Taguchi, O., Thompson, T. C., and Cunha, G. R. (1983) *J. Cell Biol.* **96,** 1671–1676
14. Cunha, G. R., Sekkingstad, M., and Meloy, B. A. (1983) *Differentiation* **24,** 174–180
15. Guo, L., Degenstein, L., and Fuchs, E. (1996) *Genes Dev.* **10,** 165–175
16. Tash, J. A., David, S. G., Vaughan, E. D. E., and Herzlinger, D. A. (2001) *J. Urol.* **166,** 2536–2541
17. Qiao, J., Uzzo, R., Obara-Ishihara, T., Degenstein, L., Fuchs, E., and Herzlinger, D. (1999) *Dev. Suppl.* **126,** 547–554
18. Baker, L. A., and Gomez, R. A. (1998) *Semin. Nephrol.* **18,** 569–584
19. Min, H., Danilenko, D. M., Scully, S. A., Bolon, B., Ring, B. D., Tarpley, J. E., DeRose, M., and Simonet, W. S. (1998) *Genes Dev.* **12,** 3156–3161
20. Young, N. S., Levin, J., and Prendergast, R. A. (1972) *J. Clin. Invest.* **51,** 1790–1796
21. Sambrook, J., Fritsch, E. F., and Maniatis, T. (1989) *Molecular Cloning: A Laboratory Manual*, Cold Spring Harbor Laboratory, Cold Spring Harbor, NY
22. Birren, B., Green. E. D., Heiter, P., Klapholz, S., Myers, R., Riethman, H., and Roskams, J. (2000) *Genome Analysis: A Laboratory Manual Series*, Cold Spring Harbor Laboratory, Cold Spring Harbor, NY
23. Weissenbach, J., Gyapay, G., Dib, C., Vignal, A., Morissette, J., Millasseau, P., Vaysseix, G., and Lathrop, M. (1992) *Nature* **359,** 794–801
24. Thomas, R., True, L. D., Bassuk, J. A., Lange, P. H., and Vessella, R. L. (2000) *Clin. Cancer Res.* **6,** 1140–1149
25. Southgate, J., Hutton, K. A., Thomas, D. F., and Trejdosiewicz, L. K. (1994) *Lab. Invest.* **71,** 583–594
26. Bassuk, J. A., Cochrane, K., and Mitchell, M. (2001) in *Bladder Disease: Research Concepts and Clinical Applications* (Atala, A., ed), in press **AQ: O**
27. Emoto, H., Tagashira, S., Mattei, M. G., Yamasaki, M., Hashimoto, G., Katsumata, T., Negoro, T., Nakatsuka, M., Birnbaum, D., Coulier, F., and Itoh, N. (1997) *J. Biol. Chem.* **272,** 23191–23194
28. McKeehan, W. L., Wang, F., and Kan, M. (1998) *Prog. Nucleic Acids Res. Mol. Biol.* **59,** 135–176
29. Igarashi, M., Finch, P. W., and Aaronson, S. A. (1998) *J. Biol. Chem.* **273,** 13230–13235
30. Lu, W., Luo, Y., Kan, M., and McKeehan, W. L. (1999) *J. Biol. Chem.* **274,** 12827–12834
31. Miyakawa, K., Ozawa, K., Uruno, T., and Imamura, T. (1999) *Growth Factors* **16,** 191–200
32. Ohuchi, H., Hori, Y., Yamasaki, M., Harada, H., Sekine, K., Kato, S., and Itoh, N. (2000) *Biochem. Biophys. Res. Commun.* **277,** 643–649
33. Karin, M., and Hunter, T. (1995) *Curr. Biol.* **5,** 747–757
34. Altschul, S. F., Madden, T. L., Schaffer, A. A., Zhang, J., Zhang, Z., Miller, W., and Lipman, D. J. (1997) *Nucleic Acids Res.* **25,** 3389–3402
35. Gribskov, M., Luthy, R., and Eisenberg, D. (1990) *Methods Enzymol.* **183,** 146–159

AUTHOR QUERIES

AUTHOR PLEASE ANSWER ALL QUERIES 1

A—Au: The Journal guidelines state that the summary should be no longer than 200 words. At this stage, we only require that the summary fit into the left-hand column. If your summary is long enough to run over into the right-hand column, please cut text.

B—Au: changed to new company name

C—Au: addition of "the" and "an optical density" as meant? if not please clarify sentence

D—Au: changed to new company name

E—Au: hyphen or chem pt used for complexes per Jnl style

F—Au: changed to new company name

G—Au: Run in per Jnl style to avoid one sentence paragraph

H—Au: is Kerinocyte Basal Labeling Media-2 a trade name, if not please change to lower case

I—Au: definition deleted after first usage with abbr per Jnl style

J—Au: should this be 326,749-kbp?

K—Au: Most abbr such as IPTG, must be used at least 3 times in summary and 5 times in text per Jnl style

L—Au: please confirm throughout text that footnote 2 info is meant or if other authors are involved please provide new footnote

M—Au: FGFRHS not used 5 times per Jnl style

N—Au: please complete Ref. 7 with vol and page nos

O—Au: please complete ref 26 with page nos and publisher and location

P—Au: Please check the colors on the computer screen against what appears in the legends to Figs, 2,3,6-8 and amend the legends as necessary. Are the color figures acceptable for publication?

Q—Au: please provide accession number in fig legend 2 and also for footnote

R—Au: please define lane 3 in fig leg 5

AUTHOR QUERIES

AUTHOR PLEASE ANSWER ALL QUERIES **2**

S—Au: Please confirm all definitions in abbr footnote

T—Au: Authors as meant for footnote 2, if not please provide first initials and last names of those involved